Institute of Paper Science and Technology
Atlanta, Georgia

IPST TECHNICAL PAPER SERIES

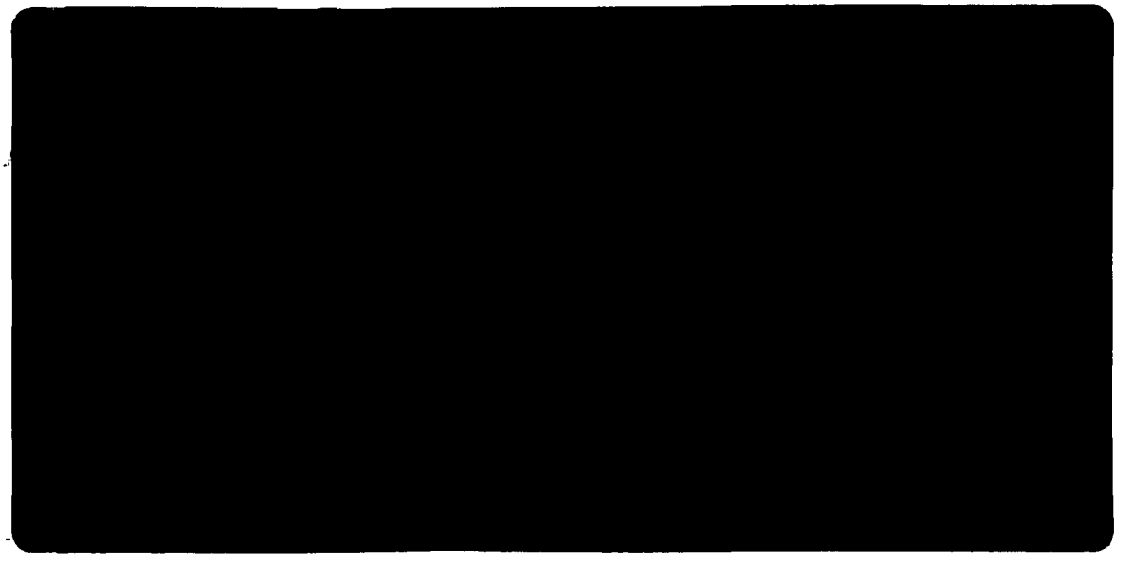

NUMBER 504

INORGANIC AEROSOL FORMATION DURING BLACK LIQUOR DROP COMBUSTION

C.L. VERRILL AND K.M. NICHOLS

NOVEMBER 1993

Inorganic Aerosol Formation During Black Liquor Drop Combustion

C.L. Verrill and K.M. Nichols

Submitted to
AIChE Annual Meeting
November 7–12, 1993
St. Louis, Missouri

INORGANIC AEROSOL FORMATION DURING BLACK LIQUOR DROP COMBUSTION

by

Christopher L. Verrill
Kenneth M. Nichols

CONTENTS

INORGANIC AEROSOL FORMATION DURING BLACK LIQUOR DROP COMBUSTION

Christopher L. Verrill
Post Doctoral Fellow
Industrial Research Chair in Pulping Technology
University of New Brunswick
Incutech Centre, PO Box 69,000
Fredericton, NB E3B 6C2
CANADA

Kenneth M. Nichols
Air Process Engineer
Weyerhaeuser Paper Company
Mailstop WTC 2F2
32901 Weyerhaeuser Way South
Federal Way, WA 98003
USA

ABSTRACT

An apparatus was developed for collection of inorganic aerosols formed during the respective stages of black liquor drop combustion. Periods of aerosol generation were coordinated with combustion events by use of a moving collection system to continuously capture the aerosol and a video camera to observe drop combustion. Time resolution of the results was limited by spatial overlap of the aerosol on the collection media. However, these experiments demonstrate that a maximum in fume formation occurred during the char burning and smelt oxidation stages of combustion. SEM photomicrographs provide further qualitative evidence that sodium release prior to char burning is not a significant source of submicron-sized fume.

Analysis of video images indicated that, throughout all stages of drop combustion, bits of liquor or char were ejected by erupting gases. A portion of this material was collected as 1-100 μm inorganic aerosol during drop combustion experiments. This size range of aerosol has been overlooked in prior studies of black liquor combustion. We feel it may contribute significantly to furnace fouling, particularly in the generating section.

INTRODUCTION

Three distinct stages of black liquor combustion have been identified: drying, devolatilization, and char burning.[1] Black liquor is introduced into the recovery furnace through one or more nozzles that produce a spray of 0.5-5 mm drops.[2] A significant portion of drying and devolatilization occurs as the drops fall to the char bed at the bottom of the furnace; much of the char burning takes place on the char bed. Under certain conditions drops can be entrained in the gas flow and burn in flight. Airborne drops exhibit a fourth

combustion stage: oxidation of the residual smelt.[1] The extent to which the combustion processes occur on the char bed and in flight depends on furnace design, liquor properties, and operating strategy.

The submicron-sized inorganic aerosol generated during kraft black liquor combustion is known as dust or fume. Fume particles are composed primarily of Na_2CO_3, Na_2SO_4, NaCl, and the equivalent potassium salts. Furnace dust samples indicate that about 10% of the sodium in the black liquor is vaporized and becomes fume.[3] The principal benefit of fume formation is that the alkali aerosol reacts with environmentally undesirable sulfur compounds in the flue gas; the resulting Na_2SO_4 dust is removed by the electrostatic precipitator and returned to the system by mixing with the black liquor. Fume has detrimental effects on recovery furnace operation because it deposits on the heat transfer surfaces which reduces thermal efficiency, requires process steam to remove the deposits, and contributes to blockage of gas passages.

Fume generation has historically been attributed to sodium vaporization from the high temperature and strongly reducing environment of the char bed.[4] Laboratory data from molten salt studies showed that the rate of fume formation is an order of magnitude higher during sodium sulfide oxidation than the rate under reducing conditions.[5] Entrained char particles and smelt droplets are exposed to an oxidizing atmosphere; therefore, they may be a significant source of fume. Experimental data indicate that sodium loss is continuous throughout combustion.[6,7,8] Furthermore, recent work has suggested that sodium release during devolatilization may contribute to overall fume formation.[8,9]

With the exception of fume formation during smelt oxidation, the relations between sodium loss and inorganic aerosol formation have not been adequately explained. The goal of this study was to determine the history of aerosol formation throughout the stages of drop combustion by measuring the amount of material collected as a function of combustion progress. Results obtained indicated that the majority of submicron-sized fume is formed during the char burning and smelt oxidation stages of drop combustion. Another category of inorganic aerosol, 1-100 μm in diameter, is thought to arise from ejection of bits of material during all stages of black liquor combustion. We suggest the use of the term *ejecta* to describe this fraction of particulate matter.

EXPERIMENTAL

During the dynamic aerosol collection experiments described in this report, drop combustion events were recorded on videotape while a moving collection medium simultaneously captured the generated particulate. Knowing the speed of the moving medium and the reactor residence time, it was possible to coordinate the timed-observation of drop combustion with the analysis of collected material, thereby creating a history of aerosol formation throughout the respective stages of drop combustion.

Drop Furnace

The drop furnace was designed to study the combustion of individual black liquor drops in a simulated recovery furnace environment. Details of the drop furnace system and its performance are discussed elsewhere.[10] Observations of drop combustion in the furnace were recorded on videotape. The video camera operated at 30 frames per second. Times for each stage of drop combustion were calculated from the elapsed time

indication on the video images. The first appearance of the drop in the field of view was used to denote the start of drying. The first sign of swelling or ignition indicated the onset of devolatilization. The maximum swollen volume of the char particle was taken as the start of char burning. Coalescence of a smelt bead denoted the start of smelt oxidation. Visible cooling of the smelt was taken as the end of drop combustion. These definitions imply that drying, devolatilization, char burning, and smelt oxidation are distinct and sequential stages of combustion; in reality, there is always some overlapping of the physical processes occurring during drop combustion.[11]

Aerosol Collection

Two equipment configurations were utilized for capturing aerosols generated during drop combustion: static and dynamic collection. In static collection experiments, the aerosol was accumulated on a small area of a stationary collection medium. In dynamic collection, the material was distributed over a relatively large area of a moving collection medium.

The aerosol collection system design was based on the use of Whatman EPM-2000 borosilicate glass fiber (BGF) filters as the collection medium. This material was chosen for its high operating temperature limit, high filtration flow capacity, and relatively low cost. Silver membrane filters, manufactured by Poretics Corp., were found to be a more suitable aerosol collection medium. This material combines the desirable characteristics -- high purity and surface capture -- of polymeric screen membranes with the superior strength and thermal stability of BGF filters.

A schematic of the dynamic aerosol collection system is shown in Fig. 1. For each dynamic aerosol collection experiment, an individual drop of industrial kraft black liquor was formed on a nichrome wire and inserted into the reaction chamber of the furnace. At the moment the drop entered the reaction chamber, a remote switch activated the fume capturing apparatus. The aerosol collection medium was mounted on a carriage that moved over the furnace exit. A constant carriage linear speed of 25.40 $\pm$ 0.02 cm/min was maintained by a dc adjustable-speed reversing drive.

The nominal combustion environment in the quartz reaction chamber was 750°C with a gas mixture of N_2 and O_2 flowing at an average velocity of 0.61 m/s. House air was mixed with compressed technical grade nitrogen to produce the desired gas composition. Gas purification chambers, packed with Ascarite II™ and Drierite®, removed CO_2 and water vapor from the house air supply.

In a typical determination, 15-25 cm of the aerosol collection medium was exposed to combustion products. Fume component assays and scanning electron microscopy (SEM) were utilized for locating aerosol deposits on the collection media. Small samples were cut from precise locations on some media and investigated by SEM. This visual observation provided qualitative information about the morphology, size distribution, and density of collected aerosols. JEOL model JSM-6400 and JSM-35C microscopes were used to investigate aerosol samples. Both microscopes were equipped with a Link Analytical LZ-4 EDS unit. Energy dispersive X-ray spectrometry (EDS) was used for qualitative determination of aerosol composition.

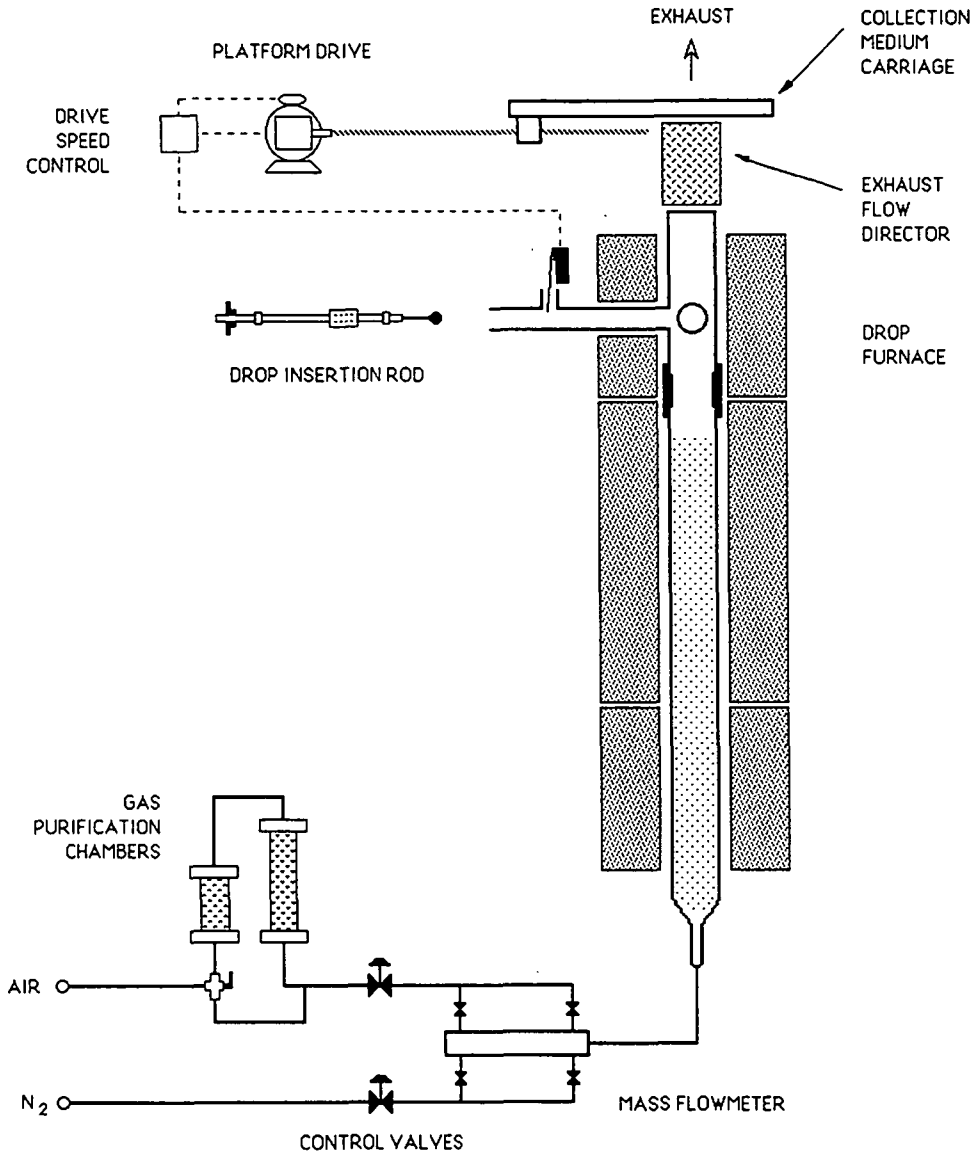

Figure 1. Schematic of experimental system used for dynamic aerosol collection.

For fume component measurement on silver membrane filters, the media were carefully divided into eight 1.3-cm sections. All filter sections and drop residues were placed in individual 50-ml centrifuge tubes and agitated in ultrapure water to dissolve the

captured inorganic compounds. Inductively coupled plasma emission spectrometry (ICP) was used to measure sodium concentration of the solutions. Anions species were measured by suppressed ion chromatography (IC). Potassium salts form a small, but significant, portion of recovery furnace fume. Potassium was not considered during this investigation of aerosol formation largely because the potassium content of a single liquor drop or collected aerosol sample was very close to the analytical detection limits.

RESULTS AND DISCUSSION

Drop Combustion Behavior

Liquor drops were fixed in place in a flowing gas stream in the drop furnace. Convection was necessary to rapidly carry any generated aerosol to the collection surface, the resulting combustion stage overlap was accounted for by careful analysis of the video images. The events observed during drop combustion, at 750°C in environments containing from 7.5 to 21% O_2, were similar to what has been described in the literature.[1,6,12,13]

In all cases we observed a brief period of drying which exhibited pronounced bubble bursting. While the trailing edge of the drop was still bubbling, the leading edge began to swell and ignition flashes were seen along the surface. Swelling proceeded rapidly to the downstream side of the particle as the volatiles flame appeared and the glow of char burning was seen on the leading edge. Bright sparks occasionally erupted from regions of the particle undergoing char burning. This material was ejected radially and at high initial velocity. Occasionally the sparks were seen to turn and follow the gas flow. In most instances it appeared that they collided with the quartz reactor tube walls.

After extinction of the volatiles flame, there were a few seconds of heterogeneous char burning, characterized by a shrinking diameter and a gaseous combustion "halo." As carbon burnout progressed tiny droplets of molten smelt formed on the upstream side of the char particles. This process occurred at all combustion conditions with more than 5% O_2. Most of the droplets of smelt disappeared into the char residue or collapsed into what appeared to be a molten smelt layer on the char surface. Some of the depending droplets detached from the char and dropped out of the field of view. This process is referred to herein as smelt shedding. When very little of the char remained, surface tension forces drew the smelt together into a single bead.

Under certain conditions material was ejected from the molten smelt bead after coalescence had occurred. This "sparking" phenomenon was suppressed if the furnace environment contained less than 10% oxygen. Two distinct periods of sparking were noted during drop combustion in air (21% O_2). In all cases there was a period of intense sparking immediately following smelt coalescence; for some drops a stream or cloud of haze persisted until the residue began to visibly cool.

Aerosol Collection on Stationary Filters

Borosilicate glass fiber (BGF) filters were initially used as the aerosol collection medium. These filters were found to be unsuitable for quantitative analysis of inorganic aerosol; however, they worked well for investigating the morphology of captured particulate in the static collection experiments. The photomicrographs presented herein are indicative of the material found during extensive searches of random samples cut from the BGF filters. No evidence of the fine particles, shown in the following photomicrographs,

was seen on the unexposed filters.

Static Aerosol Collection During Combustion

In the first static collection experiment, BGF filters were located approximately 19 cm above the drop combustion location. Filters were held in place by suction on a PTFE vacuum flow distributor; the vacuum source was a small reciprocating pump. Individual drops of liquor (63% dry solids content) were burned in air at 750°C with an average gas velocity in the reaction chamber of 0.61 m/s. Three 5 mm square samples were cut from a filter for SEM analysis.

Several large 5-20 μm spheres and numerous small 0.1-0.5 μm irregular deposits are visible in Fig. 2. The higher magnification of Fig. 3 reveals there was uniform deposition of fine aerosol on the filter fibers. The large spheres undoubtedly resulted from the ejection of bits of burning char and molten smelt, which was observed during the char burning and smelt oxidation stages of combustion.

As it was expected that the flow restriction of the reciprocation vacuum pump limited collection efficiency, the experiment was repeated after a high capacity Piab pneumatic vacuum source had been installed. Initial filter vacuum flow was varied from 100% of the gas mass flow (33 slpm*) to the low level used in the previous experiment (14 slpm). All of the samples scanned showed the presence of aerosol; EDS indicated that the composition of the particulate was primarily sodium and sulfur. Numerous 5-20 μm rough-surfaced spheres were distributed on and among the sintered fume deposits on all of

* Standard l/min; standard conditions: 20°C and 1 atm.

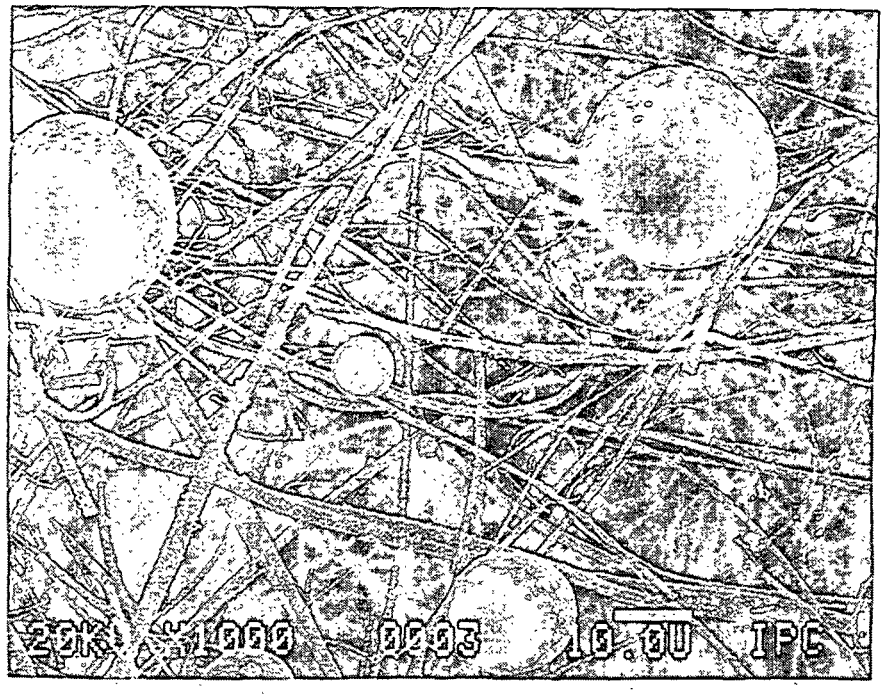

Figure 2. SEM photomicrograph showing bimodal size distribution of aerosol on BGF filter. Combustion of 27.1 mg drop in air at 750°C and 0.61 m/s; 14 slpm vacuum flow. Magnification 1,000 ×.

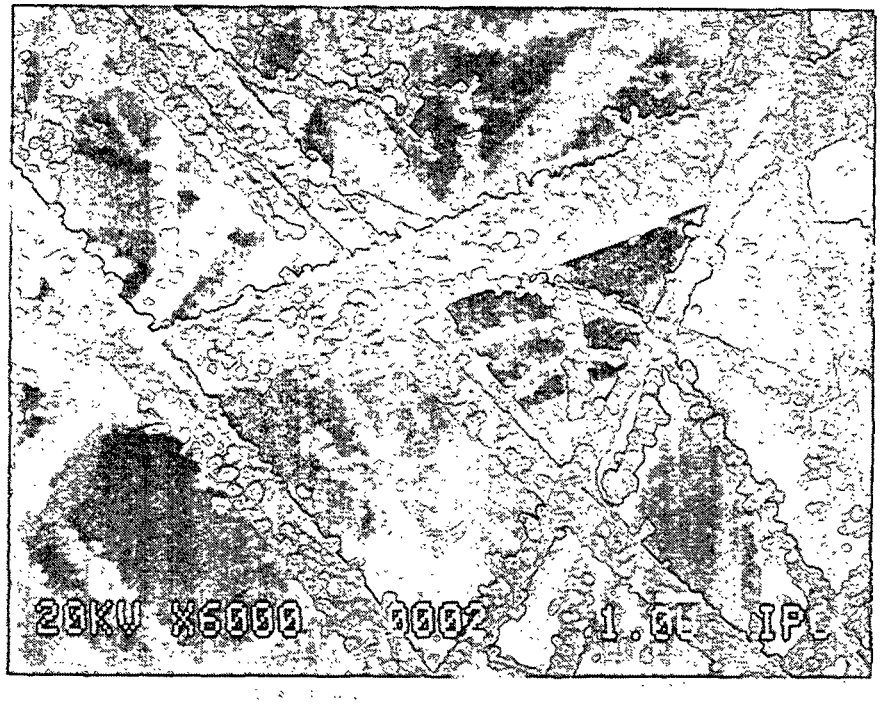

Figure 3. SEM photomicrograph showing submicron-sized aerosol on BGF filter fibers. Conditions given in Fig. 2. Magnification 6,000 ×.

the filter samples.[10] The extent of sintering suggests that the temperature at the filter was higher than in the previous trial. No effect of the initial level of vacuum flow could be determined by comparing the SEM images.

After the dynamic aerosol collection system was installed (described in the Experimental section) an experiment utilizing fixed BGF filters was conducted for comparison of collected material to the above images. A BGF filter was mounted on the carriage and held in place over the furnace exit while a 8-12 mg liquor drop was burned in air at 750°C. Gas flow rate was adjusted to produce an average gas velocity of 0.15 to 0.61 m/s in the quartz reactor tube; vacuum flow was correspondingly set at 0 to 14 slpm. The large opening of the new vacuum flow director did not restrict the vacuum flow during sampling, as had the PTFE vacuum flow distributor. The collection surface was now located approximately 32 cm above the drop combustion location. Four 5 by 5 mm samples were cut from the center region of each of five filters for SEM investigation.

There was a sparse but uniform coverage of 0.1-1.0 μm irregular fume and a few 10 μm spherical particles evident on all of the filters exposed in this experiment. Furnace gas velocity was 0.31 m/s during the collections shown in Figs. 4 and 5. Analysis of material captured at 0.61 m/s in the same experiment revealed a similar morphology to that shown in Fig. 4. The large and small particles seen in Figs. 4 and 5 resemble those found in preliminary experiments (Figs. 2 and 3); however, the density of the deposits is much less. The filters were 13 cm further away from the burning drop in the latter case. Aerosol entrainment calculations confirm that the amount of material collected should diminish with increasing distance of the filters above the drop location.[10]

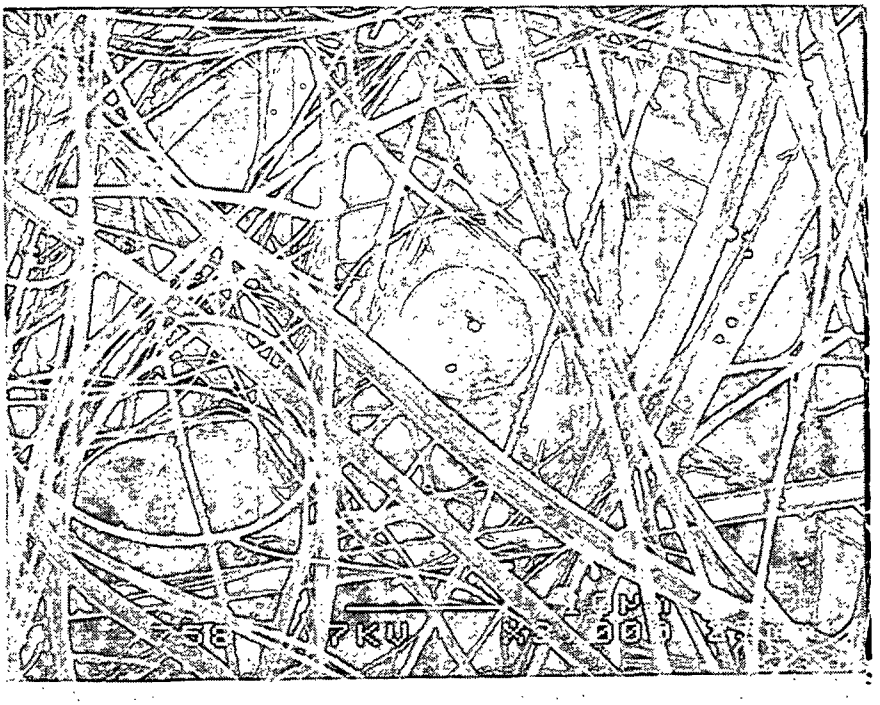

Figure 4. SEM photomicrograph showing aerosol on BGF filter. Combustion of 6.2 mg drop in air at 750°C and 0.31 m/s; 0 slpm vacuum flow. Magnification 2,000 ×.

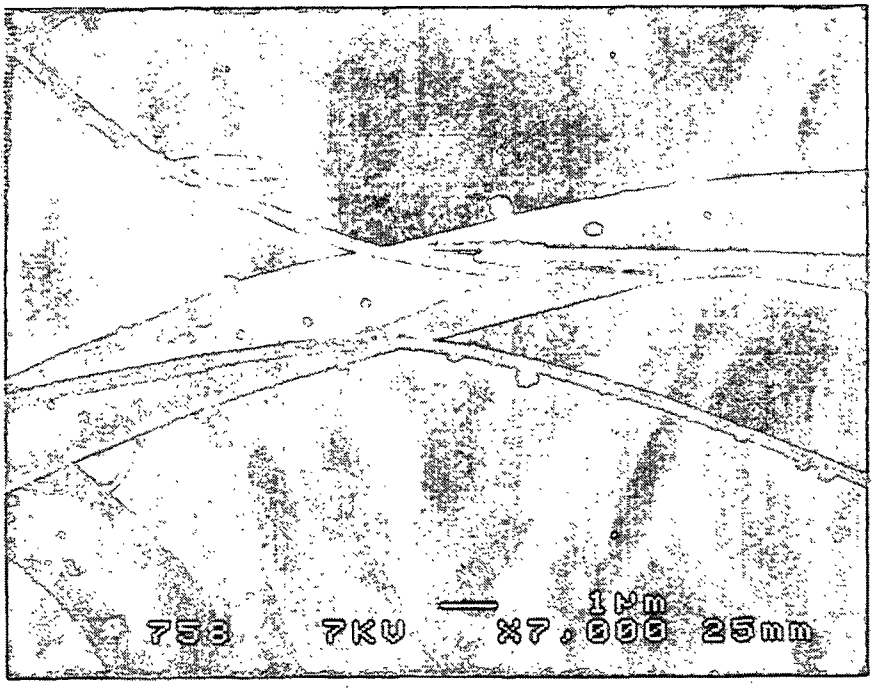

Figure 5. SEM photomicrograph showing submicron-sized aerosol on BGF filter fibers. Conditions given in Fig. 4. Magnification 7,000 ×.

Static Aerosol Collection During Pyrolysis

During several determinations of sodium mass loss during devolatilization, described elsewhere,[10,14] aerosols generated during liquor pyrolysis were collected on BGF filters. The dynamic aerosol collection system was used to place a BGF filter over the drop furnace exit. The filter remained in place during the first five individual drop exposures of each determination. Before additional drops were pyrolyzed, the collection medium carriage was activated to carry the filter past the exhaust flow. A nominal vacuum flow of 14 slpm was maintained for all static aerosol collections during pyrolysis experiments except for the trial at 750°C; in that instance there was no induced flow.

Figure 6 is an example SEM photomicrograph of the collected material from liquor pyrolysis at 900°C in 95% N_2 with 5% CO. Numerous 0.2-1.0 μm scale-like deposits and submicron-sized globular deposits are visible on the fibers. A few 10-20 μm smooth-surfaced spheres were observed on other filter samples. Deposits of the fume-like aerosol appeared to be concentrated on the surface fibers. Thermogravimetric analyses of black liquor chars, reported by Li and van Heiningen,[7] suggest that the fume collected on the filters during pyrolysis at 900°C resulted from Na release during Na_2CO_3 decomposition.[14]

Despite similar sodium mass loss values, there were fewer and less substantial 0.2-1.0 μm deposits found on the filters exposed during liquor pyrolysis at 600 and 750°C. Figure 7 is a typical representation of what was found at these conditions; little or no fume-like material was evident at 5,000 $\times$ magnification. At 10,000 $\times$ magnification, particles smaller than 0.1 μm were seen on surface of the glass fibers. While not shown in these figures, a few large (25 μm) smooth spheres and some irregular agglomerated deposits were

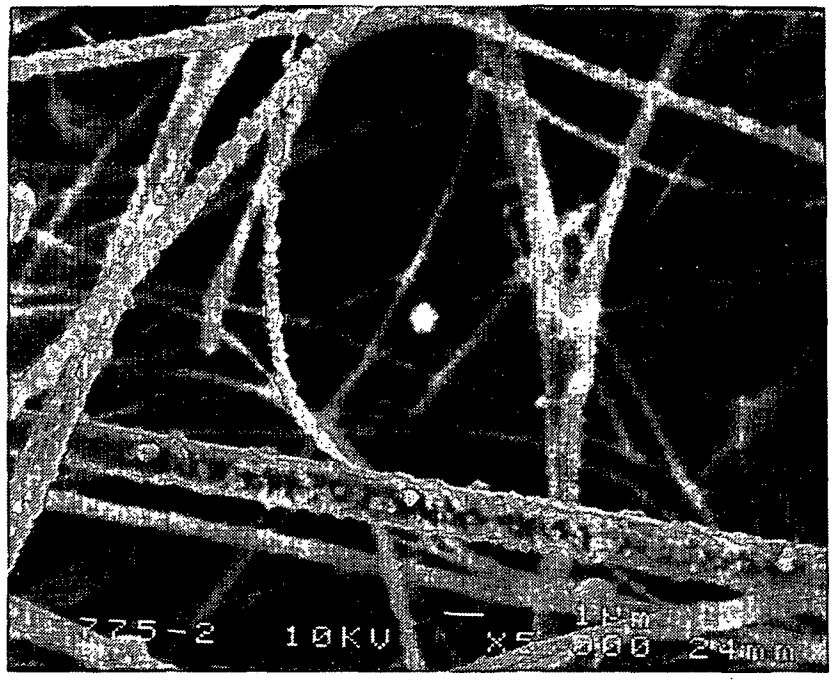

Figure 6. SEM photomicrograph showing aerosol on BGF filter. 10 s pyrolysis of 5 drops (18.9 mg total) in 95% N_2/5% CO at 900°C and 0.61 m/s. Magnification 5,000 ×.

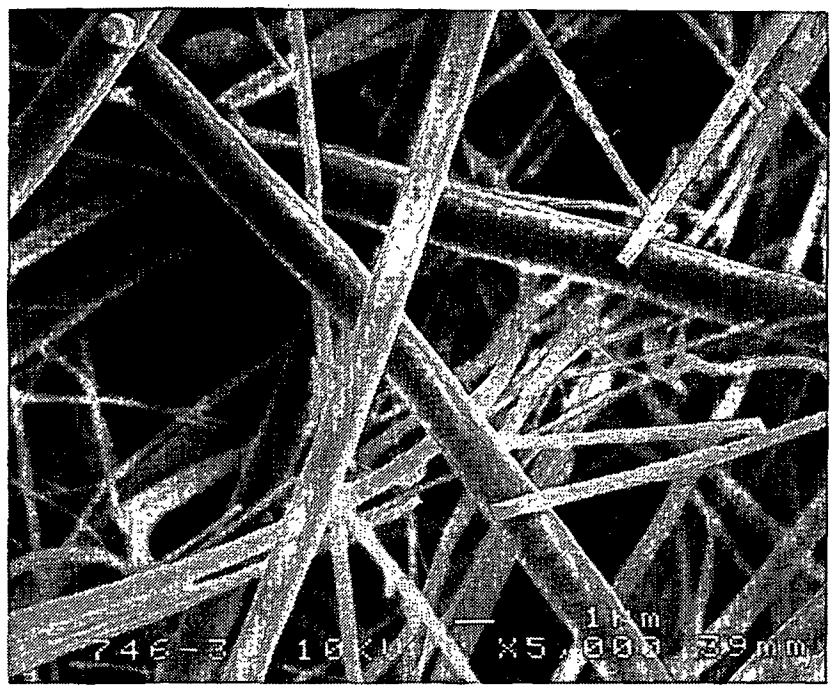

Figure 7. SEM photomicrograph showing no apparent fume on BGF filter. 10 s pyrolysis of 5 drops (24.4 mg total) in 95% N_2/5% CO at 750°C and 0.61 m/s. Magnification 5,000 ×.

observed on some regions of the filters produced during these experiments. Gasification of liquor drops at 500°C in 95% N_2 with 5% O_2 produced somewhat more 0.2-1.0 μm fume than did pyrolysis at 750°C; however, the majority of the material collected during the gasification experiment was very similar to the fine aerosol (< 0.1 μm) obtained during pyrolysis at 600 and 750°C.[10]

Comparing Fig. 7 with Fig. 5 indicates that less fume was collected during the pyrolysis of 5 drops as during the combustion of a single drop of the same liquor at 750°C. We believe these SEM photomicrographs provide qualitative evidence that less submicron-sized aerosol was formed during pyrolysis at temperatures below 900°C than during combustion in air at 750°C. This result confirms the hypothesis that sodium release prior to char burning is not a significant source of fume formation in the recovery furnace.[14] It may be argued that the released sodium would not have been collected as fume during the pyrolysis experiments if it had escaped as sodium vapor. Clearly, the presence of oxygen during liquor gasification at 500°C should have created condensed fume from sodium vapor, as described by Cameron.[15] While there was some fume-like material collected during the gasification experiment, there was more material collected on the filters from pyrolysis at 900°C in a nonreactive atmosphere. It is therefore unlikely that material escaped the collection system as alkali vapor.

Sodium mass loss during the determinations represented in Figs. 6 and 7 ranged from 20.0 to 23.0%. Interestingly enough, the *minimum* sodium mass loss measured from single drops of liquor burned in 92.5% N_2 with 7.5% O_2 at 750°C was 7-9%. These selected drops were observed not to shed any smelt beads during char burning or smelt

oxidation.[10] This agrees remarkably well with field data of Borg et al.[3] that indicate total sodium loss from the lower furnace is 9% of that fired with the liquor.

It has been proposed that physical ejection of sodium containing material is responsible for the sodium loss observed during drop pyrolysis.[10,14] However, there was little physical evidence of this material collected on BGF filters and silver membranes. The experimental system was designed to collect submicron-sized material; it is therefore expected that most of the larger aerosol was lost within the drop furnace. Due to fogging of the observation port, the quartz tube was replaced after approximately 360 individual drops had been pyrolyzed or burned at various conditions.[10] The most dense deposits, slightly above the port elevation, appeared to result from ejected material spattered on the walls.

Dynamic Aerosol Collection

In the previous section, all of the total particulate matter generated during the course of combustion was collected on a small area of filter. The technique of determining the times during combustion when different inorganic aerosols were generated required coordinating drop combustion progress with continuous collection of the aerosols as they were produced. Two successful dynamic aerosol collection experiments were conducted utilizing silver membranes as an impaction surface. Accurate determination of microgram quantities of sodium was possible with silver membranes because the levels of soluble contaminants in the membranes were extremely low. The quantity of extractable sodium was approximately 5.3×10^{-3} mg per gram of silver membrane material, as compared to a value of 16.5 mg Na per gram of the BGF filter material.

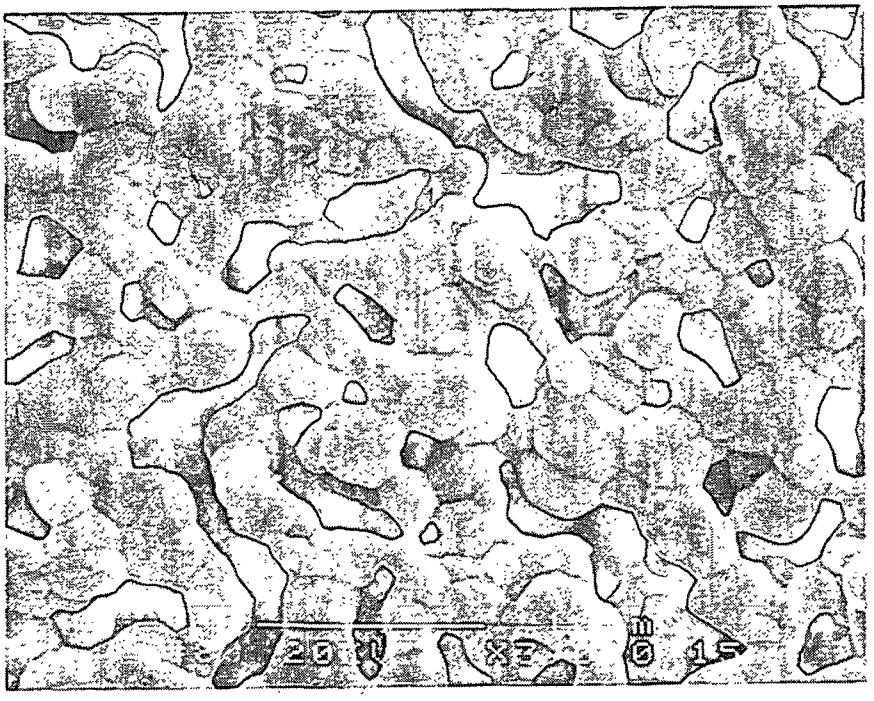

Figure 8. SEM photomicrograph showing submicron-sized aerosol on silver membrane. Combustion of 7.6 mg drop in 92.5% N_2/7.5% O_2 at 750°C and 0.61 m/s. Magnification 3,000 ×.

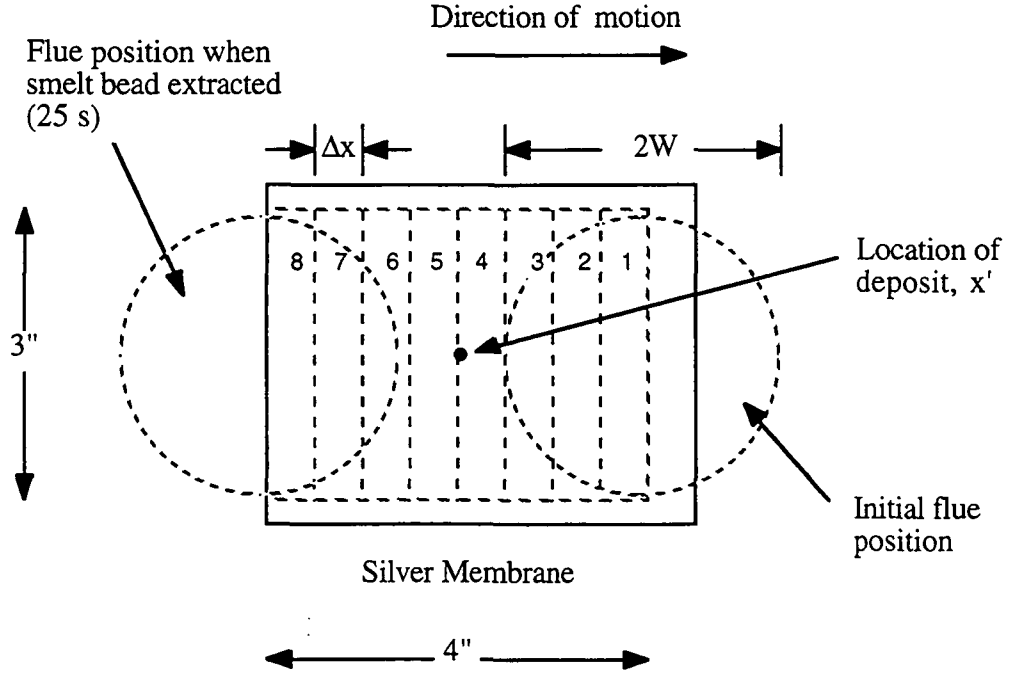

Figure 9. Schematic of silver membrane showing locations of analyzed sections and reference points for discussion of time-resolution.

SEM Analysis of Aerosol Collected on Silver Membranes

Performance of the silver membranes was evaluated in one exploratory trial using the dynamic aerosol collection system. A single 7.6 mg drop of liquor was burned in 92.5% N_2 with 7.5% O_2 at 750°C. A carriage speed of 30.48 cm/min was chosen to expose as much of the membrane as possible to combustion products. Eight consecutive samples were cut from the center line of the exposed membrane. A traverse along each sample in the direction of motion represented approximately 2.5 seconds of elapsed combustion time.

SEM analysis revealed 0.10-0.25 μm fume on all samples. Figure 8 shows that this material is similar to that observed during the static aerosol collection experiments described in the previous section. These fine white specks were not observed on unexposed sections of silver membrane. There were no large spheres (1-30 μm) found on the silver membrane samples. Deposit density was observed to increase over the first six samples and then remain constant. The overwhelming presence of silver precluded elemental analysis of the collected material by EDS.

Time-Resolution of Dynamic Filtration Data

Drop combustion exhaust gas was impacted on two moving silver membranes; additional pieces of membrane were exposed only to the hot gases to provide blank samples. After exposure each membrane was divided into eight 1.3-cm sections, as indicated in Fig. 9, and agitated in 45 ml of ultrapure water. The measured species concentrations are given in Table 1. Amounts of sulfate and chloride ions are not reported in Table 1 because they were at or below the IC detection limits. The carbonate in the two blank 1.3-cm sections was higher than in any of the exposed sections; this analysis was not repeated for the

Table 1. Analysis of silver membranes from dynamic aerosol collection experiments.

Membrane section	14.1 mg drop Na,[a] mg/L	14.1 mg drop $CO_3^{=}$,[b] mg/L	14.3 mg drop Na,[a] mg/L
1	0.04	1.16	0.12
2	0.12	1.34	0.08
3	0.10	1.58	0.08
4	0.14	1.44	0.18
5	0.16	1.42	0.30
6	0.26	1.53	0.26
7	0.18	1.72	0.21
8	0.09	1.67	0.11
Average	0.14	1.48	0.17
Detection limit	0.01	1.00	0.01
Mean background	0.04	2.13	0.04

[a] ICP analysis by Huffman Laboratories, Golden, CO.
[b] IC analysis by Institute of Paper Science and Technology, Atlanta, GA.

second experiment. If all of the collected material were Na_2SO_4 or NaCl, then the mean $SO_4^{=}$ concentration would have been 0.23 mg/l and Cl^- would have been 0.17 mg/l, about twice the detection limits for these anions. If 100% of the sodium were in the form of Na_2CO_3, the expected concentration of $CO_3^{=}$ would have been only 15% of the detection limit. Since the actual material collected was probably a mixture of these salts, sodium was the only measurable compound for this experiment.

The collection time (t_x) of an inorganic aerosol deposit, located a given displacement (x′) from the leading edge of the silver membrane depicted in Fig. 9, can be

calculated by

$$t_x = \frac{x'}{s_l} \quad , \tag{1}$$

where s_l is the linear speed of carriage. When analyzing an area corresponding to time t_x, material collected at t_x was measured but also a fraction of the material collected at all other times the cylindrical flue opening was under the point on the membrane corresponding to t_x. This region of potential overlap is $x' \pm W$ in Fig. 9. The time resolution (δ) is set by the width and shape of the flow director opening:

$$\delta_C = \pm \frac{W}{s_l} \quad , \tag{2}$$

where δ_C is the time resolution for a circular opening and W is the half-width or radius of the flue. For this experiment the time resolution was 9 seconds. The width of each membrane section (Δx) was 1.3 cm; therefore, the time interval represented by a filter segment ($t_{\Delta x}$) was 3 seconds.

Time during combustion when the sodium-containing species were formed (t_{DC}) was estimated from the locations of the membrane sections, the speed of the carriage drive mechanism, and a calculated average residence time (Θ) between drop and collection surface:

$$t_{DC} = t_x - \Theta \quad . \tag{3}$$

Residence time was calculated from a steady-state heat transfer model described elsewhere.[10] For these experiments, reactor dynamics was not the factor limiting the time resolution of the results. The estimated residence time was 1.0 s for an average gas

velocity of 0.61 m/s at 750°C in the drop reactor. This time lag was less than 5% of the mean duration of drop combustion; a small error compared to the uncertainty arising from spatial overlap of the collected aerosol on the filter.

If a spark, ejected during char burning, followed the center streamline of the exhaust gases, it would strike the membrane at $x = s_l (t_{DC} + \Theta)$. Due to mixing in the exhaust flue, the ejected particle could strike the filter anywhere within the spatial range of the flue opening ($x \pm W$). The temporal uncertainty of determining the origin of instantaneous combustion events from filter analysis is therefore $\pm W/s_l$; exactly the same as the time resolution for this geometry.

Fume Formation Rate During Drop Combustion

The rate of sodium deposition is plotted against elapsed drop combustion time in Fig. 10. Rate of deposition was calculated from the mass of sodium collected during each 3 second time interval (corresponding to the 1.3-cm sections of the membrane). Mass of sodium collected on each section of the membranes was calculated from the measured concentrations given in Table 1 minus the mean background level from the blanks. Drop combustion time, corresponding to each membrane section, was calculated by Eq. 3. The horizontal bars in Fig. 10 indicate elapsed combustion stage times with the 9 second temporal uncertainty added and subtracted from either end of the actual stage time ranges.

The entrainment and collection efficiency calculations described below indicate that submicron-sized fume should have been collected preferentially to larger aerosol on the silver membranes. Therefore, the sodium deposition rate history shown in Fig. 10

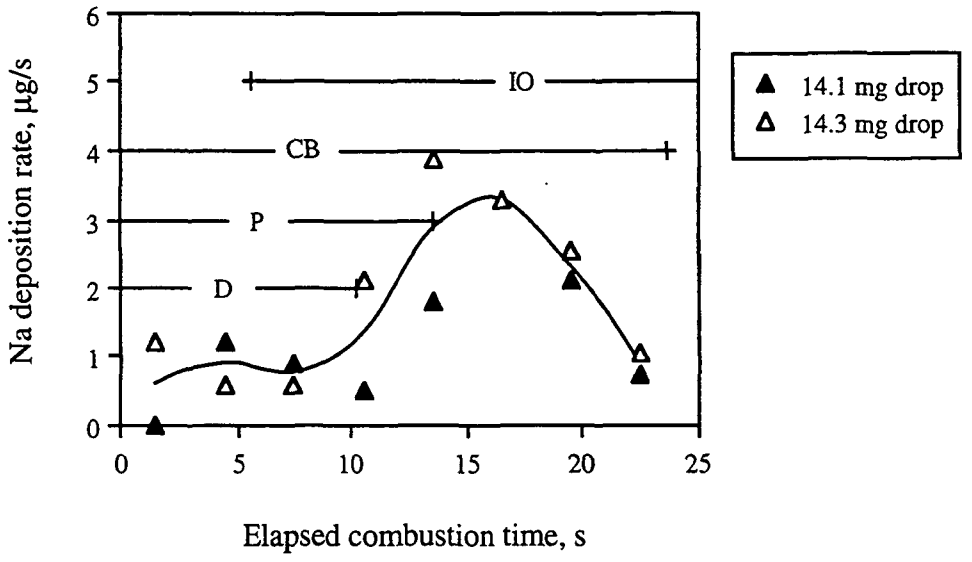

Figure 10. Sodium deposition rate from dynamic collection experiment; combustion in 7.5% O_2/92.5% N_2 at 750°C. Bars show stage times: D - drying, P - devolatilization, CB - char burning, IO - smelt oxidation.

approximately represents the rate of fume formation. This important result demonstrates that maximum sodium release, leading to fume formation, occurred during the char burning and smelt oxidation stages of combustion. The primary inorganic product during this phase would have been Na_2CO_3 as there should be no oxidized sulfur gases evolved after the completion of devolatilization.

Observations of combustion in 7.5% O_2 at 750°C and the results of the dynamic aerosol collection experiments suggest that there were two potential phases of aerosol formation during combustion at these conditions. The first phase occurred during the overlapped devolatilization and char burning stages, possibly producing Na_2CO_3/Na_2SO_4 fume and inorganic ejecta. The second phase extended from char burning through smelt oxidation and produced primarily sodium carbonate fume and ejecta. At high enough oxygen partial

pressure there would have been a third phase of aerosol generation resulting from sparking during smelt coalescence. This phase would have produced 20-100 μm sized particles characterized by typical smelt composition.

Aerosol Entrainment

During the drop combustion experiments, the mass flow of gas was adjusted to produce a desired average gas velocity at the set temperature of the quartz reaction chamber. Gas velocity decreased as a result of progressive cooling with displacement past the top of the drop reactor heating elements. Entrained material would have fallen out of the gas stream when its settling velocity exceeded the upward gas velocity ($u_t = u_{max}$).[2] The critical velocity necessary to determine the maximum size of the material reaching the aerosol collection plane is therefore the gas velocity at the exit of the exhaust flow director.

For low particle Reynolds number, $Re_p < 1$, and small particle size, $d_p \approx 10$ μm, inertial forces acting on a body are negligible compared to viscous forces. For this so-called Stokes' law range, the terminal or settling velocity of spherical particles in still air (u_t) is given by

$$u_t = \frac{g}{18} \frac{d_p^2 \rho_p}{\mu} \quad , \tag{4}$$

where g is the gravitational acceleration constant, ρ_p is particle density, and μ is gas viscosity. Gas density is very much larger than ρ_p and was therefore assumed to be negligible in this formulation. Appropriate correction factors extend the range of particle size for which Stoke's law calculations are valid to $0.2 < d_p < 100$ μm.[16]

During all aerosol collection experiments there was laminar flow in the drop reactor; assuming that a fully developed laminar profile was maintained within the exhaust flow, then the maximum upward velocity equalled twice the average velocity ($u_{max} = 2\langle u \rangle$) at any axial displacement. We assumed that the majority of generated aerosol followed the central "core" of gas flowing at between maximum and average velocity. Equation 4 was rearranged to calculate maximum entrainable particle size (d*e*). For the region of interest, $\langle u \rangle \leq u_t \leq u_{max}$,

$$de = \sqrt{\frac{18\, u_t\, \mu}{g\, \rho_p\, C_c}} \quad , \tag{5}$$

where C_c, the Cunningham correction factor, accounts for the reduced resistance of viscosity as particle size approaches the mean free path of the gas. Assuming that the maximum entrainable particle size is greater than 10 μm, $C_c = 1.0$ may be used with little error.[17] Exit velocity was predicted by a steady state heat transfer model.[10]

Table 2. Calculation of maximum entrainable particle size at given locations for dynamic aerosol collection experiments.

Location	d*e* @ $\langle v \rangle$, μm	Re_p @ $\langle v \rangle$	d*e* @ v_{max}, μm	Re_p @ v_{max}
Drop plane	136	0.67	193	1.9
Exit plane	57	0.36	80	1.0

Table 2 contains the values of d*e* calculated for the aerosol collection experiments. A typical smelt density value was chosen as the density of inorganic aerosol ($\rho_p = 2.5$ g/cm^3).[2] For all cases, the assumptions of Stokes' law behavior and $C_c = 1.0$

were valid because $Re_p < 2$ and $10\ \mu m < d_p < 100\ \mu m$. SEM analysis of collected aerosol indicated that most particles were spherical in shape; slight irregularities in shape would not be expected to cause significant error in the Stokes' law calculations.[16]

It can be concluded from this analysis that particles larger than 0.1-0.2 mm (smelt ejecta, shedded smelt droplets) fell to the bottom of the furnace, and that particles smaller than 57-80 μm reached the silver membrane.

Collection Efficiency on Silver Membranes

When a particle-laden gas stream encounters a fixed object, submicron-sized particles will tend to follow the streamlines of the gas flowing around the object. Particles greater than 1 μm in size have sufficient inertia to prevent them from following streamlines when a flow suddenly changes direction. Depending on their size and velocity, they may collect on the immersed object by either interception or impaction. Interception occurs when the particle comes within one particle radius of the collecting surface.

The minimum particle size with sufficient inertia to be collected by impaction is greater than 150 μm, for the conditions of the dynamic aerosol collection experiment. In Table 2, d*e* was calculated to be less than 80 μm at the exit plane; clearly there would have been no aerosol collection by impaction on the silver membranes. Theoretical collection efficiency, however, does not necessarily accurately represent the true efficiency of aerosol capture.[18] In the above analysis only the mechanism of impaction was considered. As the exhaust flow contacted the surface of the silver membrane there may have been submicron-sized aerosol collection by electrostatic attraction and diffusion.[16] Loss of aerosol after

contact by reentrainment after contact is unlikely for particles smaller than 10 μm because the adhesive forces that act on the particle are two orders of magnitude greater than the removal force of a 10 m/s air current.[17]

During the aerosol collection experiments, the relative change in sodium content from the original liquor to the smelt residue was 25-48%. It is not certain how much of the sodium loss was in the form of fume and how much was as shed smelt droplets; however, it is expected that only a fraction of the airborne material was collected on the silver membrane. Between 5 and 7% of the total sodium "lost" during drop combustion could be accounted for on the silver membranes; we consider this an indication of the minimum collection efficiency. Assuming 8% of the sodium present in the liquor became fume, total sodium loss for these drops was partitioned into vaporized and shed fractions.[10] This calculation suggests that the maximum collection efficiency would have been 22-29%.

The range of 6-25% collection efficiency for the silver membranes does not seem unreasonable for this experiment. There was no collection of large particles because the minimum particle size necessary for inertial impaction was substantially larger than the maximum expected to be carried to the collection plane. Only submicron-sized aerosol would have been light enough to be collected by electrostatic forces or diffusion as the exhaust flow contacted the silver membrane surface. This conclusion is supported by the absence of large particles ($d_p > 1$ μm) in SEM images of silver membrane samples (Fig. 8).

Aerosol Formation During Drop Combustion

Although the final composition of fume is approximately 90% Na_2SO_4 and

10% Na_2CO_3, it is unlikely that fume originates from direct vaporization of these species. The vapor pressure of pure Na_2SO_4 is 2.7 x 10^{-2} Pa at 980°C.[19] At the same temperature the vapor pressure of Na_2CO_3 is approximately 11 Pa.[20] Advanced equilibrium calculations indicate that elemental sodium vapor, NaOH, and NaCl are the primary sodium species in the gas phase above the char bed.[21] The vapor pressures of these compounds at 980°C are at least four orders of magnitude higher than Na_2SO_4.[2] Fume must therefore originate from gas phase reactions of volatile alkali species to form condensed products.

Fume formation in the kraft recovery furnace was first attributed to sodium vaporization from the reducing environment of the char bed.[4] A condensed fume species (Na_2O) was thought to form just above the bed, where the reactive metal vapor first encountered oxygen. Researchers at the Institute of Paper Chemistry found that when oxygen-containing gas was contacted with molten salt systems an order of magnitude more fume was produced than under reducing conditions.[5] The measured rate of "oxidative" fume formation was much greater than that estimated by assuming that equilibrium sodium vapor pressure had been established. Cameron[15] proposed a reaction-enhanced mechanism of fume formation, wherein rapid oxidation of sodium vapor near the smelt surface reduces the partial pressure of sodium in the boundary layer. The resulting increase in driving force enhances the rate of sodium vaporization.

Frederick and Hupa[8] suggested that sodium release during devolatilization may be the most significant source of fume. Their justification was that the amount of sodium evolved during single drop pyrolysis was an order of magnitude higher than that released during char burning and smelt oxidation. This amount of sodium could account for the total

mass of fume collected in the electrostatic precipitator. However, our SEM photomicrographs indicate that little submicron-sized fume was formed during the pyrolysis experiments. Only at temperatures high enough for Na_2CO_3 decomposition to occur were substantial quantities of fume collected. Our drop furnace was not designed to collect large aerosol; appearance of the combustion chamber after numerous drop exposures and entrainment calculations indicate that most of this material was lost within the system. However, calculations showed that collection efficiency for submicron-sized aerosol was reasonably high. Results of dynamic aerosol collection on silver membranes indicated that the majority of the sodium collected as fume was released during the char burning and smelt oxidation stages of black liquor drop combustion.

Physical Ejection

During the first observations of spent liquor drop combustion in laboratory furnaces, researchers noted that the drops bubbled violently during drying.[1,12,13] Bubble formation and erupting jets of gases were also observed in photographic images of devolatilizing black liquor solids.[22] The eruptions of water vapor and pyrolysis gases from the surface film of the liquor drops would eject tiny droplets of liquor into the gas phase surrounding the particle. Physical transport of sodium-containing material, ejected during drying and devolatilization, may explain sodium loss during the single drop pyrolysis experiments. The reported effect of heating rate supports this hypothesized mechanism.[14]

It is not certain if physical ejection of sodium-containing material produces submicron-sized fume in recovery furnaces. Under noncombustive conditions, organic alkali compounds in the ejecta would rapidly decompose to low molecular weight gases and sodium

carbonate aerosol. If the gaseous environment supported combustion, then the mechanisms of char burning and smelt oxidation would produce sodium vapor from the burning bits of ejected liquor.[2,15] Sodium vapor would further react with O_2, H_2O, and CO_2 in the gas phase and condense as fume. The fate of ejected matter must be considered in a global furnace environment. It could be entrained and produce fume; however, it could also deposit on other liquor drops and heat transfer surfaces or fall to the char bed.

A Third Category of Particulate

From limited furnace aerosol collection studies, it has been established that fume and carryover are two distinct types of solid material that reach the heat transfer surfaces in the recovery furnace.[23,24,25,26] Results of our work suggest that a third category, ejecta, should also be considered. Furnace particulate samples have been found to contain a fraction of 1-100 μm inorganic aerosol.[24,27] This was postulated to result from entrainment of smelt beads remaining at the end of airborne drop combustion.[27] Smelt beads should be about half the initial diameter of liquor drops (0.25 - 2.5 mm);[2] therefore, the collected particles were too small to support the stated hypothesis.

It is more likely that the large aerosol originated as ejecta. During the early stages of drop combustion bits of liquor and char are ejected by erupting gases. If smelt coalescence occurs in regions of high oxygen concentration, then numerous smelt droplets are ejected by escaping CO_2. This material has been overlooked as an important aspect of furnace chemistry and fouling. The electrostatic precipitator catch from overloaded suspension-fired boilers contains a substantial amount of inorganic material larger than 10 μm.[28] At the higher gas velocity within the generating bank, these larger particles may

deposit on boiler tubes by inertial impaction.[29] Analysis of furnace dust samples from this region should verify the presence of this intermediate-sized inorganic aerosol.

CONCLUSIONS

Inorganic aerosols were collected during the respective stages of black liquor drop combustion. Time resolution of the results was limited by spatial overlap of the aerosol on the collection media. However, the measured sodium deposition history was representative of submicron-sized fume formation from a burning drop. Results of these experiments demonstrate that a maximum in fume formation occurred during the char burning and smelt oxidation stages of combustion.

SEM photomicrographs showed that more submicron-sized fume was produced during the combustion of a single drop of black liquor than during the pyrolysis of five drops at similar furnace conditions.

There was evidence of physically ejected material during all drop combustion stages. Much of this material deposited on the reactor tube walls during our experiments. Within the kraft recovery furnace, the ejecta may react to produce fume, collide with other airborne particles, fall to the char bed, or deposit on furnace heat transfer surfaces.

The aerosol collection experiments provided important information regarding the nature of inorganic aerosol formation during drop combustion. Additional experiments are required to isolate the fume from the ejected material. The dynamic aerosol collection system can be utilized to collect fume on silver membranes. Another technique must be developed to independently capture the ejecta.

An industrial furnace study should be directed towards size classification of inorganic aerosol, and determination of the role of ejecta in fouling. A multistage low pressure cascade impactor would best be utilized to isolate the various aerosol size fractions.[30] Such a study would also provide data for validating a computational model of the aerosol mechanics and chemistry within the kraft recovery furnace.

ACKNOWLEDGEMENTS

Funding for this work was provided by the Institute of Paper Science and Technology and its member companies. Dr. John Cameron is gratefully acknowledged for initiating the investigation. Dr. Lisa Detter-Hoskin is thanked for her skillful assistance with the SEM. Portions of this work were used by C.L. Verrill as partial fulfilment of the requirements of the degree of Doctor of Philosophy at the Institute of Paper Science and Technology.

LITERATURE CITATIONS

1. Hupa, M.; Solin, P.; Hyöty, P., Combustion behavior of black liquor droplets. J. Pulp Paper Sci. 13(2):J67-72 (1987).

2. Adams, T.N.; Frederick, W.J., Kraft Recovery Boiler Physical and Chemical Processes. The American Paper Institute, New York (1988).

3. Borg, A.; Teder, A.; Warnqvist, B., Inside a kraft recovery furnace - studies on the origins of sulfur and sodium emission. Tappi 57(1):126-129 (1974).

4. Lang, C.J.; DeHaas, G.G.; Gommi, J.V.; Nelson, W., Recovery furnace operating parameter effects on SO_2 emissions. Tappi 56(6):115-119 (1973).

5. Clay, D.T.; Grace, T.M.; Kapheim, R.J., Fume formation from synthetic sodium salt melts and commercial kraft smelts. AIChE Symposium Series 80(239):99-106 (1984).

6. Volkov, A.D.; Evseev, O.D.; Ibatullina, R.I.; Dravolina, E.I., Sodium loss during burning of moist particles of black liquor. Mezhuz. Sb. Nauchn. Tr. Ser. Khim. Teknol. Tsellyul. (7):72-75 (1980). *Translation available from the Institute of Paper Science and Technology.*

7. Li, J.; van Heiningen, A.R.P., Sodium emission during pyrolysis and gasification of black liquor char. Tappi 73(12):213-219 (1990).

8. Frederick, W.J.; Hupa, M., Evidence of sodium fuming during pyrolysis of black liquor. Tappi 74(11):192-194 (1991).

9. Frederick, W.J.; Forssén, M.; Hupa, M.; Hyöty, P., Sulfur and sodium volatilization during black liquor pyrolysis. Proc. TAPPI/CPPA Int. Chem. Recovery Conf., Seattle, WA, p. 599-608 (1992).

10. Verrill, C.L., Inorganic aerosol formation during black liquor drop combustion. Ph.D. Dissertation. Institute of Paper Science and Technology, Atlanta, GA (1992).

11. Frederick, W.J., Combustion Processes in Black Liquor Recovery: Analysis and Interpretation of Combustion Rate Data and an Engineering Design Model. Report No. One of U.S. Dept. of Energy, DOE/CE/40637-T8 (DE90012712) (March, 1990).

12. Monaghan, M.T.; Siddall, R.G., The combustion behavior of waste sulfite liquor - a preliminary investigation. Tappi 46(2):89-91 (1963).

13. Björkman, A., Pyrolysis of spent liquors. Proc. IUPAC/EUCEPA Symp. Recovery of Pulping Chemicals, Helsinki, Finland, p. 235-267 (1968).

14. Verrill, C.L.; Grace, T.M.; Nichols, K.M., The significance of sodium release during devolatilization on fume formation in kraft recovery furnaces. J. Pulp Paper Sci., in press (1993).

15. Cameron, J.H., Reaction enhanced vaporization of molten salt. Chem. Eng. Comm. 59:243-257 (1987).

16. Fuchs, N.A., The Mechanics of Aerosols. Pergamon Press, Macmillan Co., New York (1964).

17. Hinds, W.C., Aerosol Technology: Properties, Behavior, and Measurement of Airborne Particles. John Wiley and Sons, New York (1982).

18. Davies, C.N., Deposition from moving aerosols. Aerosol Science. Davies, C.N., ed. Academic Press, New York, p. 393-446 (1966).

19. Kohl, F.J.; Stearns, C.A.; Fryburg, G.C., Sodium sulfate: vaporization thermodynamics and role in corrosive flames. NASA Technical Memorandum NASA

TM X-71641. Presented at the Electrochem. Soc. Int. Symp. on Metal-Slag-Gas Reactions and Processes (1975).

20. Andresen, R.E., Solubility of oxygen and sulfur dioxide in molten sodium sulfate and oxygen and carbon dioxide in molten sodium carbonate. J. Electrochem. Soc. 126(2):328-334 (1973).

21. Pejryd, L.; Hupa, M., Bed and furnace gas compositions in recovery boilers - advanced equilibrium calculations. Proc. Tappi Pulping Conf., San Francisco, CA, p. 579-590 (1984).

22. Miller, P.T., Swelling of Kraft Black Liquor. An Understanding of the Associated Phenomena During Pyrolysis. Ph.D. Dissertation. The Institute of Paper Chemistry, Appleton, WI (1986).

23. Bosch, J.C.; Pilat, M.J.; Hrutfiord, B.F., Size distribution of aerosols from a kraft mill recovery furnace. Tappi 54(11):1871-1875 (1971).

24. Nguyen, X.T.; Rowbottom, R.S., Characterizing particulates from kraft recovery boilers. Pulp Paper Can. 80(10):T318-T324 (1979).

25. Reeve, D.W.; Tran, H.N.; Barham, D., The effluent-free bleached kraft pulp mill - Part XI. Pulp Paper Can. 82(9):T315-T320 (1981).

26. Rizhinshvili, G.V.; Kaplun, L.V., Means to reduce furnace emissions of soda recovery boilers. Bumazh. Prom. (1):26-28 (1983). *Translation available from the Institute of Paper Science and Technology.*

27. Tran, H.N.; Reeve, D.W.; Barham, D., Formation of kraft recovery boiler superheater fireside deposits. Pulp Paper Can. 84(1):T7-T12 (1983).

28. Samuelsson, I.L.; Bradburn, K.M., Electrostatic precipitator design and operation, to meet particulate emission control requirements, for today's trends in recovery boiler operation. Information presented at TAPPI/CPPA Int. Chem. Recovery Conf., Seattle, WA (1992).

29. Goerg, K.A., A Study of Fume Particle Deposition. Ph.D. Dissertation, The Institute of Paper Chemistry, Appleton, WI (1989).

30. Kauppinen, E.I.; Pakkanen, T.A., Coal combustion aerosols: a field study. Environ. Sci. Technol. 24(12):1811-1818 (1990).